Proceedings of the Institute of Acoustics

ON HIGH TECHNOLOGY AND HIGH FREQUENCY SEAFLOOR ACOUSTICS

AP Lyons The Pennsylvania State University, Applied Research Laboratory, P.O. Box 30, State College, PA 16804, USA

1 INTRODUCTION

Knowledge of scattering by and penetration into sediments is required for accurately predicting the performance of modern high-frequency military and civilian acoustic remote sensing systems. High-frequency systems, such as those used for seabed characterization or object detection, have been operated under the assumption that, due to the prohibitively high compressional wave attenuations within the sediment volume, seafloor returns are almost exclusively caused by scattering from the rough water-sediment interface. Also assumed is that past the critical angle, penetration of the acoustic field into the sediment is negligible, thereby excluding the possibility of detecting buried targets. Recent studies have challenged both of these common assumptions, with sediment volume scattering shown to be dominant in some cases above 100 kHz[1,2], and energy observed on buried hydrophones at subcritical grazing angles[3,4].

Studies designed to examine high-frequency seafloor scattering or penetration mechanisms have been limited by the difficulty of accurately characterizing seabed properties at millimeter scales. Both the two-dimensional interface controlling roughness scattering and the three-dimensional internal structure of the top tens of centimeters of seafloor sediments controlling volume scattering require accurate measurement tools that are non-destructive and that have high spatial resolution. Subcritical penetration mechanisms have not been satisfactorily explained to date due to ambiguities in traditional buried hydrophone measurement systems in addition to the lack of two-dimensional seafloor roughness measurements. Recently, tools for addressing these experimental shortfalls have been developed to support seafloor acoustics measurements, and information obtained from these systems is being used to address many open questions in high-frequency seafloor acoustics. This paper provides a review of the development and use of several non-traditional technologies in seafloor acoustics studies including: x-ray computed tomography (section 2), digital photogrammetry (section 3), and buried directional sensors (section 4).

2 ILLUMINATING HIGH-FREQUENCY SEDIMENT VOLUME SCATTERING MECHANISMS VIA X-RAY CT SCANNING

2.1 Overview

A complete description of backscattering from the ocean bottom must include scattering from the volume beneath the water-sediment interface. The volume scattering component might include discrete particle scattering and/or continuum scattering. The sediment volume matrix can be thought of as a random continuum whose properties vary randomly and continuously in space. The continuous property variations of the sediment continuum can be caused by small scale layering of the subbottom or variations in sediment water content. Discrete scatterers are random distributions of particles within the sediment volume such as bubbles, buried rocks or shells, and marine organisms or their burrows within the sediment. Spatial scales of heterogeneities, which are important to scattering, can be an order of magnitude smaller than the acoustic wavelength requiring very high-resolution descriptions of seafloor structure. The lack of high-resolution data and the lack of information about variation in the horizontal plane are fundamental problems in characterization of the seafloor interface and volume for scattering predictions.

X-ray computed tomography (CT) of cores could be used to provide three dimensional seafloor descriptions on scales smaller than 1 mm^3. This scale of description is very relevant to sediment internal volume scattering at acoustic frequencies of 10's to 100's kHz. Characterizations of these seafloor types based on the high-resolution environmental data sets can be incorporated into forward models of scattering behavior and comparisons made between the various scattering mechanisms. This section examines how X-ray computed tomography (CT) scans of seafloor cores have been used to obtain data sets that not only allow computation of both the statistical and the spatial distribution of density-related parameters relevant to volume scattering modeling, but also represent a valuable tool for selective, nondestructive 3-dimensional visual analysis of inner features of cores. The main advantages of X-ray CT are the excellent (sub-millimeter) spatial resolution and the ready availability of digital data sets that naturally lend themselves to computer processing.

X-ray computed tomography (CT) was developed during the early 1970's to generate cross-sectional x-ray images of the brain[5]. Also called computer-assisted tomography or CAT scanning, the medical community quickly demonstrated the diagnostic power of CT in the analysis of body tissues and in the detection of tumors. These studies demonstrated, however, the potential usefulness of CT in the study of marine sediments due to the technique's ability to differentiate regions of subtle density contrasts within intact sediment cores and to do so nondestructively. The fundamental property measured by CT is the linear attenuation coefficient (m) of x-ray energy. Numerous studies have verified the strong linear correlation between sediment bulk density and x-ray attenuation, usually reporting correlation coefficients greater than 0.99 (e.g., Warner et al.[6]).

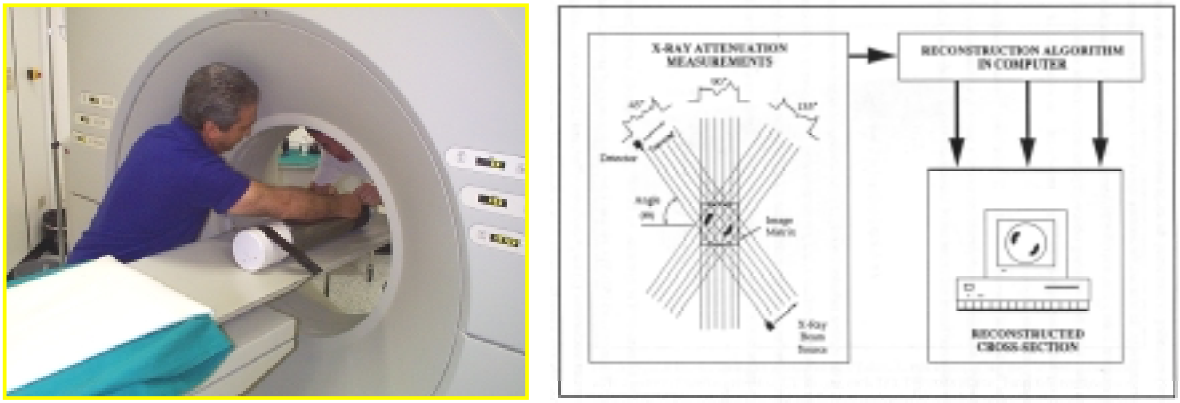

FIGURE 1. (left) Procedure employed to perform x-ray tomography on sediment cores using a medical scanner. (right) General aspects of x-ray CT. Three-dimensinal information is obtained by incrementing the sample into and out of the scan plane.

The four basic components of a CT scanner are the x-ray source, the detector array, an automatic micro positioning table, and the central control computer. The sample is centered within a circular gantry that supports the x-ray source and detectors. By rotating around the test sample (Figure 1), each source-receiver location provides a line integral measurement of x-ray attenuation. After measuring and combining over a span of locations greater than 180^o, transformation of the attenuation data by a filtered back-projection reconstruction algorithm results in a two-dimensional grid of attenuation values. The dimensions of the individual volume elements in the matrix (i.e., voxels or three-dimensional pixels) determine the spatial resolution of a CT scanner. By incrementing the sample through the scan plane using the positioning table, contiguous sections can be obtained which, when compiled via imaging software, permit three-dimensional visualization of sedimentary structures. The 3-D reconstruction in Figure 2 shows significant inhomogeneity of sediments taken at Porto Venere, Italy, due to a high degree of bioturbation.

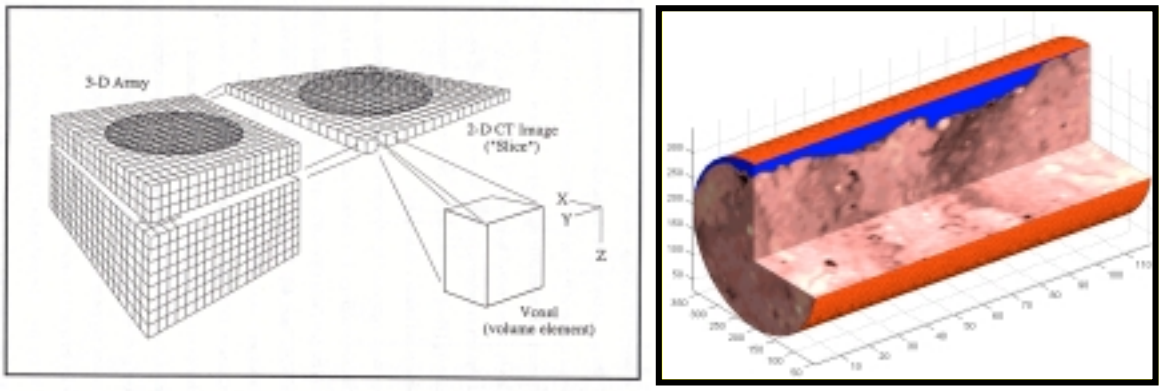

FIGURE 2. (left) Three-dimensional array of reconstructed CT data. (right) Three-dimensional Cut-away view of core formed from the density values in the data array.

Several studies of high-frequency seafloor acoustics have been performed recently using x-ray CT technology to provide high-resolution sediment volume characterization. The information provided has proven useful in constraining parameters required for high-frequency volume scattering predictions. The remainder of this section provides background on the methods used and then continues with example results including the use of x-ray computed tomography in quantifying density variability and vertical density gradients and how these data are employed to evaluate parameters that allow acoustic models to be fully constrained.

2.2 Methods

As the seafloor studies concerned were of very high frequency volume scattering (i.e. typically 10's to 100's of kHz, corresponding to centimetric to sub-centimetric acoustic wavelengths), short cores were found to be sufficient to capture enough sediment (down to several acoustic wavelengths). To reduce disturbance, cores were taken manually by divers. Most of the cores analyzed for the various studies were taken vertically although some were taken with the longitudinal axis of the core liner kept horizontal. Taking cores horizontally gave rise to some difficulties during collection and processing, the technique has the advantage of allowing scanning of the core in its natural orientation. For a vertical core this would require that it be short enough to pass through the gantry on which emitters and detectors rotate, while horizontal cores allow any liner length. In all of the studies X-ray CT scans were performed within hours after in-situ sampling to reduce compaction and decomposition. The cores were kept unopened during the entire procedure.

2.3 Examples

2.3.1 Discrete Objects

In addition to a "qualitative" visual analysis, the CT data set allows thorough "quantitative" characterization of the seabed. In the first two examples algorithms have been implemented to identify objects (a confined volume within the sediment in which physical properties differ significantly from the surrounding material) and compute their volume, which are necessary to quantify the distribution of parameters such as the "equivalent radius" (i.e., the radius of an equivalent spherical volume).

2.3.1.1 BUBBLES

In sediment regions with high organic content, a possible contributor to acoustic volume scattering has been found to be scattering from free gas bubbles within the sediment. After obtaining the cores and while still at the seafloor, divers sealed them into pressure tight aluminum transfer chambers to maintain in situ pressures. Upon retrieval to the surface and while still under pressure inside the chambers, the samples were scanned with an X-ray CT scanner[7,8]. Bubble identification and quantification were possible because of the great bulk density contrast between free gas and other constituents of the sediment. Figure 3 shows a vertical CT image of core taken in Eckernfoerde Bay, Germany. Water surrounding the core liner appears as light blue in this figure, sediment as shades of brown, and free gas features (bubbles) within the sediment as black. Sizes for equivalent radii of the features in the core ranged from 0.5 mm (the smallest feature we could detect) to about 8.0 mm. Also shown in Figure 3 is a plot of surface are ratio (the ratio of measured bubble surface areas to that of an equivalent sphere). The general trend for gas features found in Eckernfoerde sediments is for increasing non-sphericity with increasing size. Approximate methods for including the effect of non-sphericity in acoustic predictions can be found in Lyons, et al.[7] Figure 4 shows the bubble size distribution of a section of this core can be modeled with an exponential distribution, pointing out the possibility of many undetected smaller bubbles. In order to show the utility of CT scans of gassy sediment cores, a backscattered pressure time series predictions based on the measured bubble size distribution and shape estimates is also shown in Figure 4 along with experimental broadband measurements (10-35 kHz) taken at the site of the core.

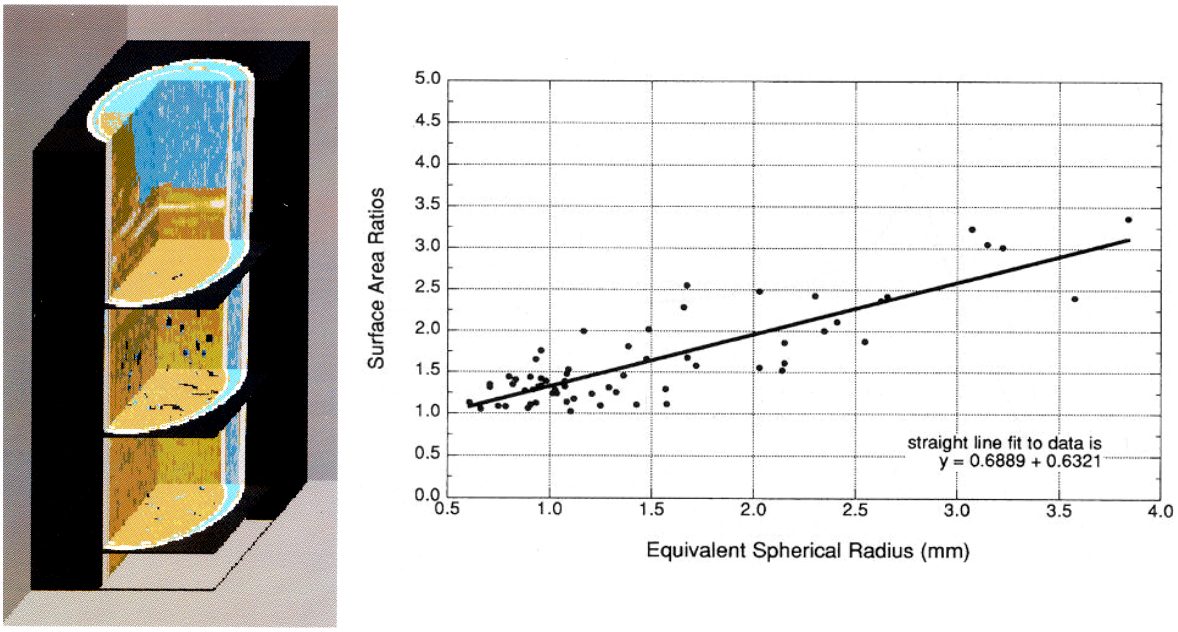

FIGURE 3. (left) Three-dimensional cut-away view of density for a core obtained at Eckernfoerde Bay, Germany. Water density values in this image are light blue, sediment values are displayed shades of brown, and values for gas features are set to black. (right) Surface area ratio as a function of equivalent radius for the core shown on the left. A surface area ratio of 1 indicates a spherical shape while larger values indicate increasingly non-spherical shapes.

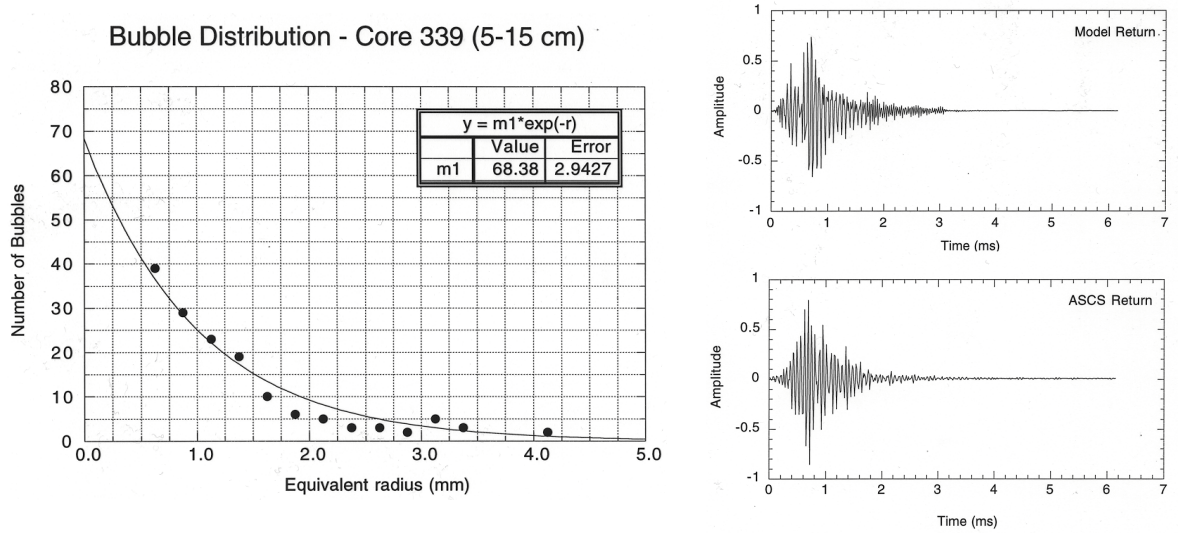

FIGURE 4. (left) Bubble size distribution estimated for the core shown in Figure 3 together with fitted exponential distribution. (right) Modeled time series of backscattering based on the bubble size distribution compared with a measured time series taken at the core location.

2.3.1.2 SHELL PIECES

A not uncommon contributor to acoustic scattering in many shallow water areas is scattering from discrete shell pieces and a very important parameter needed to describe many sediments in which there are dispersed shell fragments is the number of shell fragments per unit volume. This is not something that can be directly determined with fragile shell fragments, as a sieving process to determine size distribution has the possibility of breaking larger fragments into smaller pieces thereby distorting the estimate. The method of stereological examination of cores that had been x-ray computed tomography (CT) scanned[9] was chosen to estimate the shell size distribution in the cores presented in this example. This is possible because of the extremely thin horizontal resolution of the scanner, 0.25 mm for a vertical slice of data, and because the X-ray CT data can be directly related to values of density.

Figure 5 shows a density image (on the left) from one of two sub cores of a box core taken in Panama City, Florida, sediments. The shell pieces are evident as bright white in the colors of the sediment background. The image on the right shows the shell pieces as contours of the threshold value. It is possible to determine a distribution of sphere sizes in a matrix by measuring the size of the circular profiles cut through the spheres by the planar CT vertical sampling surface. If there are several different sizes of spheres present in the sample, a particular size circle could result from intersection of the planar section with many different sphere sizes. The frequency distributions for each size will add, giving rise to a complicated size histogram. The problem is to deconvolve this complex distribution of circle sizes into the distribution of sphere sizes, from which the mean diameter and hence the number of features per unit volume can be obtained. An approach to solving this type of problem is to solve a set of simultaneous equations to relate the sizes of spheres to the measured histograms. This solution leads to a matrix of coefficients, which can be used to multiply the number of circles in the measured histogram to obtain the corresponding distribution of spheres. The method of determining these coefficients is discussed by Cruz-Orive[10]. The graph on the left side of Figure 6 shows the real shell size distribution obtained from the profile distribution for the core shown in Figure 5 (note that the size axis is the log of the particle radius). The shape of this curve corresponds closely to a lognormal distribution described by the function

$$N(a) = \Delta + \beta \exp\left(-\frac{\left(\log(a) - a_0\right)^2}{\sigma^2} \right) \quad (1)$$

In this equation Δ is the offset, β is the peak value, a_0 is the mean and σ is the standard deviation.

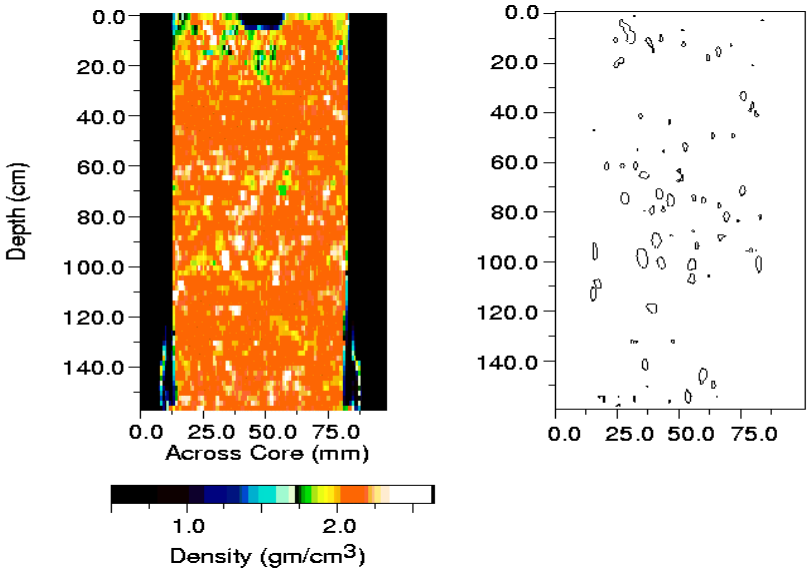

FIGURE 5. (left) Two-dimensional density image of core taken off Panama City, Florida. (right) Contours of shell pieces from the same density image.

As an example of how this distribution could be used in seafloor acoustics, the right side of Figure 6 displays the volume scattering cross section versus frequency calculated for the lognormal distribution described by Equation (1) constrained by parameters obtained from the Panama City Core. This volume scattering cross section can be included in models of seafloor scattering in a manner similar to Lyons[9].

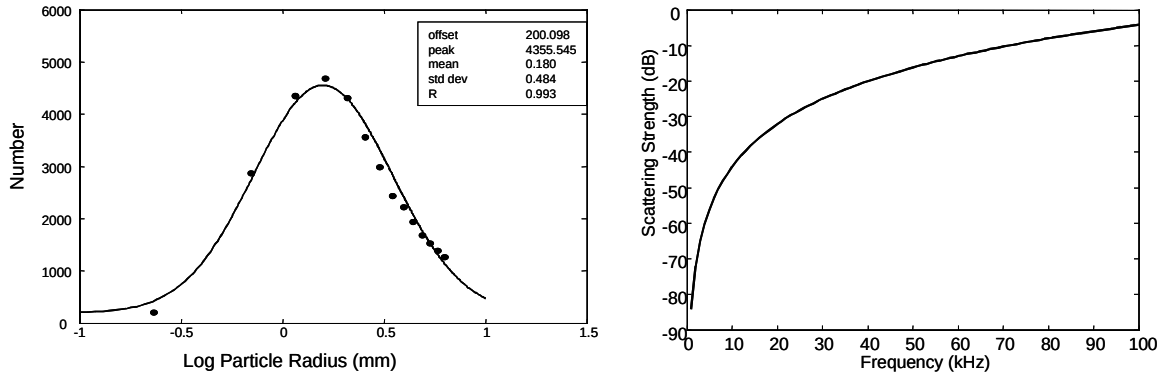

FIGURE 6. (left) Shell size distribution estimated from core taken off Panama City, Florida. (right) Volume scattering cross section calculated using the estimated shell size distribution.

2.3.2 Density Gradients

As a further example of the utility of scanned ground truth cores to high-frequency seafloor acoustics, an x-ray CT data set has been processed to investigate the variation of density with depth below the seafloor surface. Cores scanned for this example were collected near Porto Venere, Italy and were processing to allow estimates of the density profile to be obtained. . An example of the density gradient extractd from core data is shown in Figure 7 along with two sample CT scans. Divers took this core horizontally so that the scans are oriented properly. Note that the water sediment interface in the density profile in Figure 7 is offset by approximately 2 cm.

Using data collected at Eckernfoerde Bay, Germany[11], Lyons and Orsi[12] showed how naturally occurring strong variations of the density gradient with depth in the first few centimeters below the water-sediment interface affect high-frequency reflection, forward loss and backscatter. A modified power-law function was proposed to model the variation of density with depth:

$$\begin{aligned} \rho(z) &= \rho_w, && \text{for } z < 0 \\ \rho(z) &= \rho_s - \frac{\rho_s - \rho_0}{1 + az}, && \text{for } z \geq 0 \end{aligned} \tag{2}$$

The parameters of sediment asymptotic density, ρ_s, initial surface density, ρ_0 and gradient strength, *a*, that best fit profiles extracted from cores such as that shown in Figure 7 can be computed by fitting of Equation (2) to the density profiles. Comparisons between 140 kHz seafloor backscatter data and scattering predictions based on including the gradient modeled by Equation (2) can be found in Pouliquen and Lyons[1] and Muzi et al.[1]

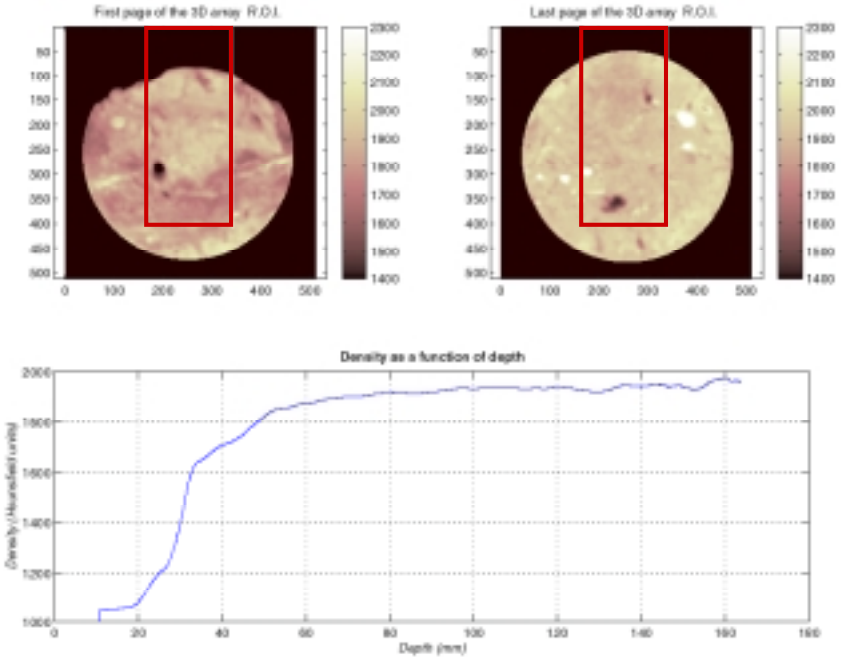

FIGURE 7. (top) Two sample density images of a core collected in soft sediments near Porto Venere, Italy. The red boxes in the images delineate areas used for extraction of the mean density profile. (bottom) Mean density profile extracted from the core. Note that the sediment-water interface is offset by approximately 2 cm.

2.3.3 Power Spectra

The random nature of seabed heterogeneity is treated in the acoustic scattering models[1,14] by means of a stochastic approach, which requires the computation of the relative density fluctuation,

$$\gamma_\rho = \frac{(\rho - <\rho>)}{<\rho>}, \tag{3}$$

and its three-dimensional power spectrum. Knowledge of the power spectrum is essential because backscattering strength is proportional to the value of the density power spectrum at the Bragg number. Processing of an x-ray CT data set allows computation of density fluctuation at the location of every single voxel, which in turn allows computation of the three-dimensional spectrum. For visualization purposes, an example of a two-dimensional core section and its associated two-dimensional spectrum is shown in Figure 8.

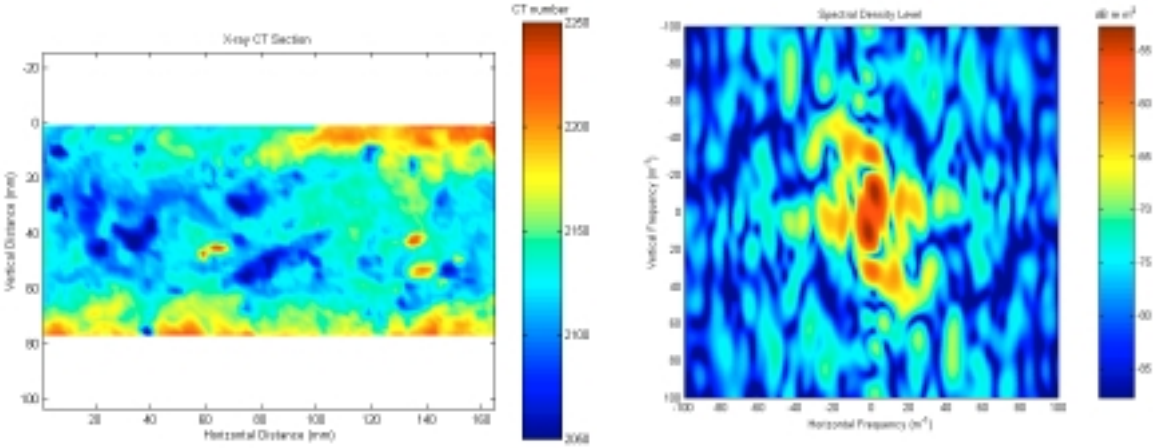

FIGURE 8. (left) Two-dimensional slice of CT number, which is directly proportional to density for a core, collected in mixed sand/silt sediments near Venere Azzura, Italy. (right) Two-dimensional spectrum estimated for the section shown at left.

If power spectra show three-dimensional isotropy of the density field, a radially averaged spectrum is adequate to represent the fluctuations and is modeled by the following expression:

$$S_{\rho|\mathrm{mod}el-3D}(k) = \frac{l_1\gamma_1}{\pi} \cdot \frac{a_1}{\left[1+(l_1 k)^2\right]^{\gamma_1+1}} \tag{4}$$

Processing the CT data set yields an experimental estimate of the radially averaged spectrum and the proper values of a_1, l_1 and γ_1 to constrain the spectrum model are obtained by fitting Equation (4) to the experimental data.

3 DIGITAL PHOTOGRAMMETRY: A NEW LOOK AT THE SEDIMENT INTERFACE FOR MODELING HIGH-FREQUENCY ROUGHNESS SCATTERING

3.1 Overview

Surface roughness is a fundamental property of the seafloor affecting a variety of physical phenomena including sediment transport and acoustic interaction with the seafloor. The amount and variety of efforts in this area are highlighted in two recent special issues of the IEEE Journal of Oceanic Engineering. Of particular interest are outstanding issues revealed during the SAX99 sediment acoustics experiment and related experiments. Measurements made during SAX99 include forward and backscatter from the seabed, acoustic propagation within the surficial sediments, and detection of buried objects at subcritical grazing angles. Some experimental results suggest that diffraction by sand ripples is a leading cause of acoustic penetration into sediments at subcritical grazing angles[15]. However, Synthetic Aperture Sonar (SAS) measurements for the detection of buried cylinders and spheres at subcritical grazing angles in the presence of ripple fields at the sediment surface yielded mixed results. While a cylinder at 50 cm depth in the sediment was always detected, a cylinder at 15 cm depth was only detected for 1 of 3 runs, and buried spherical targets were never detected[16]. In light of expectations based on previous experiments showing subcritical acoustic penetration, the inconsistent detection results were not well understood.

Repeatedly cited, as a missing link in fully interpreting and understanding the results from these experiments is a robust method for two-dimensional in situ characterization of anisotropic seafloor

roughness. What remains to be determined are the critical range of parameters for a ripple field, such as ripple height and wavelengths that yield enhanced penetration at subcritical grazing angles. Seafloor roughness is dynamic and a particular sediment surface can change on scales of days or even hours due to bioturbation. The semi-organized ripple surfaces put down by waves will be randomized by bioturbation, eventually erasing the anisotropic structures that exist[17]. Even though the surface is continually changing, the underlying statistical description or roughness spectrum has been assumed to be relatively stable. In contrast, the spectrum of roughness for rippled, shallow-water seafloors should have strong time dependence. Further, the effect of time and spatial variability of the ripple fields sue to bioturbation and hydrodynamic forcing on penetration and buried object detection needs to be understood.

A digital close-range photogrammetry system has been recently developed[17] with an image acquisition system based on the flexibility and low cost of digital cameras. The system uses stereo images of the seafloor taken with the digital cameras to produce surface elevation models in a digital format, i.e., digital elevation models (DEMs). Secondary analysis can then be carried out on the DEMs such as the estimation of height and slope distributions, estimation of two-dimensional spectra, or estimation of rms radius of curvature. Some of the advantages offered by the digital photogrammetric system over traditional analytical systems are: (1) stereo images can be acquired and measurements carried out in near real time; (2) acquired images can be displayed and used for measurements on standard computer display devices with no optical or mechanical requirements; (3) the measurement systems are stable and need no recalibration; (4) image enhancement, such as equalization, can easily be applied to the original images to facilitate later processing by increasing the dynamic range of pixel values; (5) corrected images are not necessarily required as any distortions of the images can be taken out through mathematical transformation.

3.2 Image Acquisition System

The cameras used in the system for which results are presented in this paper are inexpensive, off-the-shelf, digital cameras. In digital cameras the common solid-state imaging device known as a charge-coupled device (CCD) creates the digital images. The CCD sensor consists of a two-dimensional array of closely spaced, highly photosensitive, semiconductor elements that change light into electrical signals that are converted and encoded into digital data for digital still photography. The individual CCD elements in the sensor array are analogous to pixels in a digital image array. The CCD has the advantages of low noise, high dynamic range and good reliability at a low cost compared to other solid-state sensors. When using digital cameras for photogrammetric purposes, fiducial marks are not necessary because the regular array of light sensitive elements within the CCD image sensor can be used as a photo-coordinate system.

The two digital cameras are mounted on a frame in containers, which are watertight to 100-m depth and are connected by a serial cable to a shipboard computer for real-time acquisition of digital images (Figure 9). The exact orientation in space of the two cameras is controlled and known exactly in order to make accurate, sub-millimeter-scale photogrammetric estimates of seafloor roughness from stereo pairs. It is not usually convenient to set up the cameras with their focal axes parallel, because this limits the region of space in which objects are visible in both images. It is more favorable to aim the cameras so that their focal axes are angled inwards and converge on the seafloor patch of interest. A convergent focal geometry allows a large base-to-height ratio, which is generally required to accurately estimate the height field of seafloors that have moderate relief. A strobe or constant, high-intensity lamp was attached to the frame for use as a light source when needed for taking underwater photos in low-light conditions.

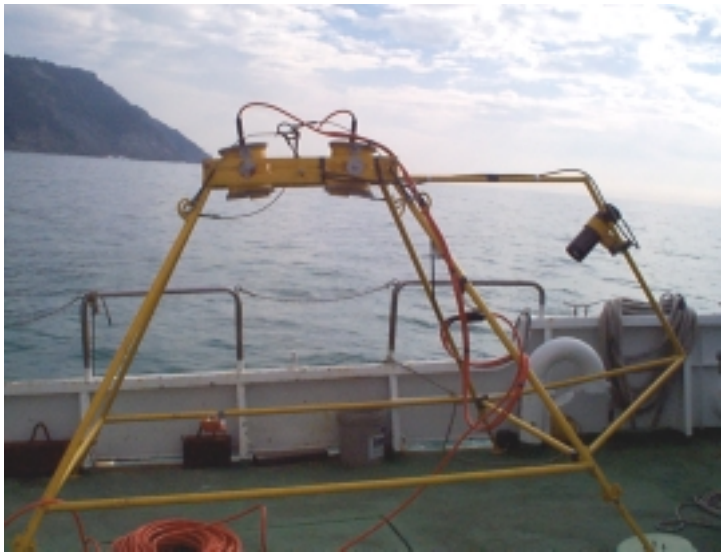

FIGURE 9. Underwater components of the digital stereo camera system. The cameras are housed in the containers at the top of the frame and a high-intensity strobe is seen at right.

3.3 DEM Production

Viewing a scene from two (or more) different positions simultaneously allows the 3-D structure to be inferred, provided that corresponding points in the images can be identified. Human visual systems make use of this fact, as do photogrammetric systems. The correspondence problem in close range digital photogrammetry concerns the matching of points in two images such that the matched points are the projections onto the image planes of the same point in the scene. Stereo disparity of the point is the difference in the horizontal positions (x-coordinates) of a particular point on the rectified (orientation corrected) images. With knowledge about the transformation between the coordinates of points for the two cameras, a map of disparity can be obtained from the matching stage that can then be used to compute the 3-D position of the scene points. The final product is the full 2-D height field, or DEM, which has several advantages to previous techniques, such as allowing the full 2-D spectrum to be estimated. Several steps are necessary, however, before the final height field can be obtained from a pair of digital photos, including image rectification and stereo-correlation. A brief overview of the steps involved in processing the stereo images is given below.

An important step in the process of DEM production is known as rectification and is the estimation and removal of the effects of relative camera orientation (Figure 10). The transformation parameters can be estimated by using known corresponding points on the two images of a stereo pair. Once the camera orientation parameters are found, the photographs are corrected pixel by pixel to remove the orientation effects and produce registered images. When a pair of stereo images is placed in register, residual differences in the horizontal image coordinates are assumed to result from relief displacement. The differences in the apparent horizontal position of the point due to changes in camera position (x-parallax) may then be used to derive relative elevations or height differences by utilizing a computational technique known as automatic stereo-correlation. A simple technique for finding corresponding points on two registered stereo images is known as area-based matching which searches a sub-window in the two images by comparing an even smaller sub-window until the correlation is maximized (Figure 11). The points that have maximum correlation are considered to be the same point on both images. The procedure is repeated for each pixel of the image until a map of the height field or digital elevation model is estimated (Figure 12).

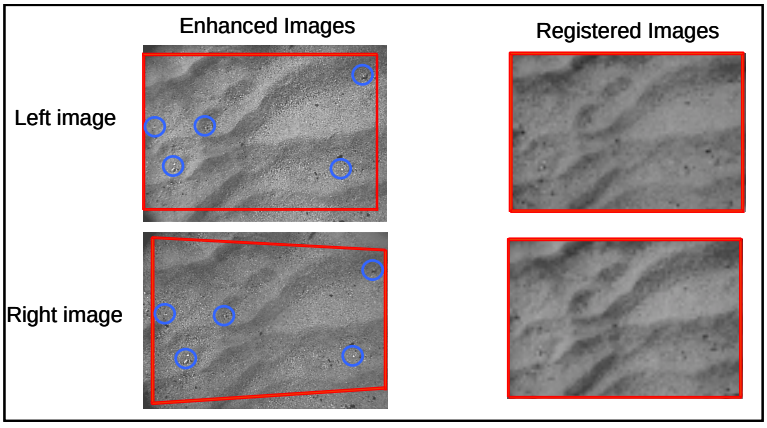

FIGURE 10. Example of image registration for the estimation and removal of the effects of relative camera orientation.

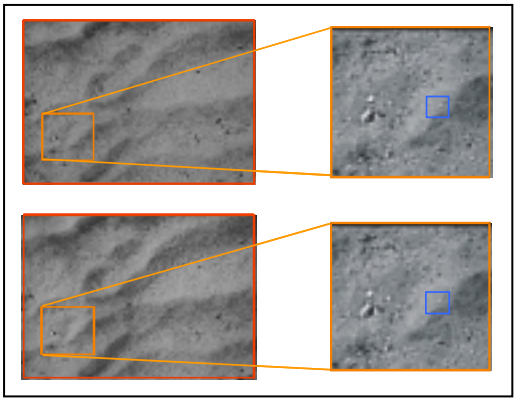

FIGURE 11. Example of stereo correlation to determine the positions of corresponding points on two registered images. Residual differences of the x-coordinates result from relief displacement and are used to derive relative elevations.

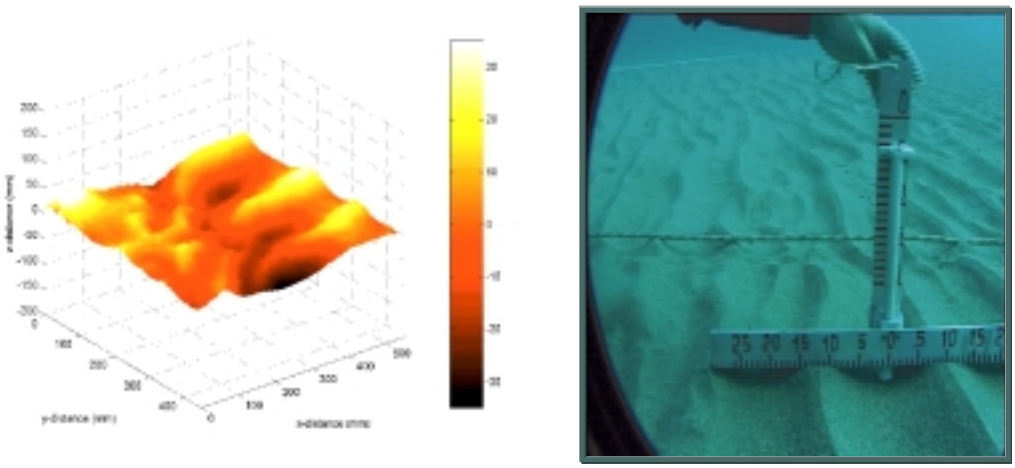

FIGURE 12. (left) Example digital elevation model (DEM) estimated for the images in Figures 10 and 11. (right) Old technology for measuring ripple characteristics serves as a check on the new.

3.4 Examples

Several seafloor scattering and penetration experiments have made use of the photogrammetry techniques (refs). Since 1997, the SACLANT Undersea Research Centre (now the NATO Undersea Research Centre) has been developing and improving a digital stereo-photogrammetry system able to retrieve two-dimensional patches of the bottom interface height of a size of about 1x2 m with a spatial sampling resolution less than a millimeter. This system has been thoroughly tested and validated in tanks on known interfaces and at sea at the occasion of more than a dozen sea trials. It has proved to be a reliable system able to provide in area of good optical visibility an accurate spatial and temporal quantification of bottom roughness as evidenced by the examples below.

3.4.1 Two Dimensional Measurements

While one-dimensional analysis should be sufficient for isotropic roughness, it can be very limiting in the study of anisotropic (e.g. rippled) seafloors such as those influencing results from the seafloor penetration and scattering experiments mentioned above. Roughness measurements in support of high-frequency seafloor acoustics studies have in the past typically relied on conventional analytical photogrammetric profiling techniques. Although it is possible to perform full two-dimensional (2-D) analysis on photogrammetrically derived sediment height values, due to the great time and effort involved in the use of conventional systems, only reduced estimates of roughness such as rms heights or one-dimensional roughness spectra are usually produced. Figure 13 gives an example of a two-dimensional height field obtained from anisotropic sandy sediments near Elba Island, Italy and its associated two-dimensional spectrum. The spectrum is characterized by quasi-periodic component seen as peaks in the low wavenumber portion of the spectrum and an isotropic power law component seen as a general falling off of level toward higher wavenumbers. The full two-dimensional spectrum for this type of anisotropic seafloor has been found to be[17]:

$$W(\mathbf{k}) = W_p(k) + W_g(\mathbf{k}). \tag{5}$$

The isotropic component, $W_p(k)$, is described by a power law of the form:

$$W_p(k) = ak^{-b}, \tag{6}$$

where k is the magnitude of the two-dimensional wave vector.

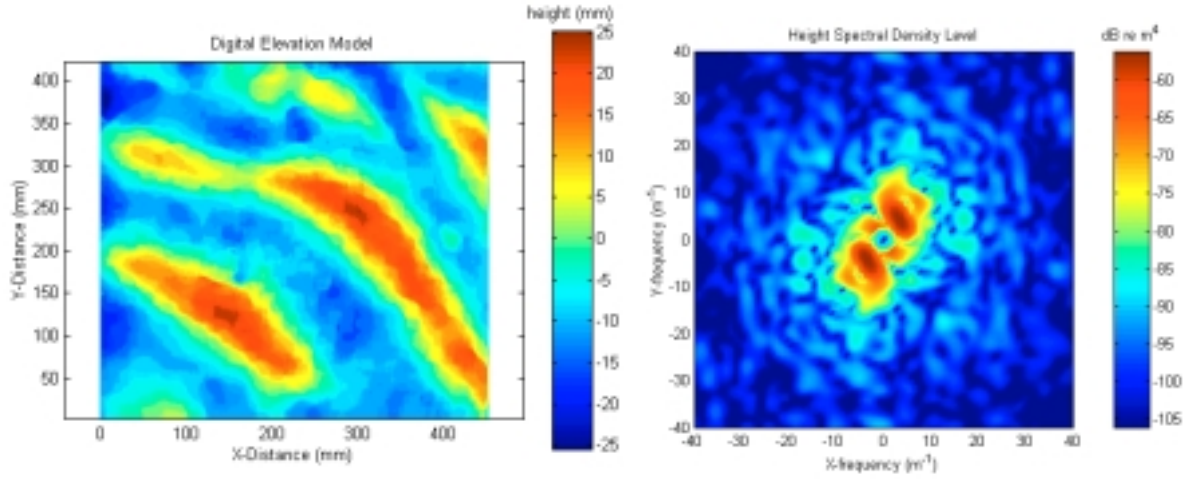

FIGURE 13. (left) Two-dimensional height field for rippled sand sediments near Elba Island, Italy. (right) Two-dimensional spectrum estimated for the height field shown at left.

The Gaussian component, $W_g(\mathbf{k})$, which describes the quasi-periodic nature of the seafloor is given by

$$W_g(\mathbf{k}) = Q(\mathbf{k},\mathbf{k}_c) + Q(\mathbf{k},-\mathbf{k}_c), \tag{7}$$

where the spatial wavenumber $\mathbf{k}_c = (k_{xc},k_{yc})$ defines the average ripple wavelength and orientation. The function Q, which is simply a shifted Gaussian form, is given by

$$Q(\mathbf{k},\mathbf{k}_c) = \frac{l_x l_y \eta^2}{4\pi} \exp\left[-\frac{l_x^2 (k_x - k_{xc})^2 + l_y^2 (k_y - k_{yc})^2}{2} \right], \tag{8}$$

with k_x and k_y being the components of wavenumber, and l_x and l_y the correlation lengths in the x- and y-directions respectively. The parameter η allows the roughness variance to be specified independently of $\mathbf{k}_c$ and is simply the rms ripple height. The strength of anisotropy is a function of $\mathbf{k}_c$, l_x, and l_y, and when $\mathbf{k}_c$ is set to (0,0) and $l_x = l_y$ the seafloor has no directional features. The distribution of power between the two components will be a function of time with the periodic component decaying and the power law component increasing as the ripples start to be reworked by bioturbation.

3.4.2 Time Evolution Studies

An interesting application of the photogrammetry system made possible by the ease of automation inherent in a fully digital system is the study of changes in roughness over an extended period of time. As discussed above, changes in roughness have the potential to make a buried object visible or invisible, for example, by erasing ripple structure and the associated diffraction of the acoustic field. As part of the SAX99 experiment at Panama City, Florida, Richardson, et al.[18] have recently analysed changes in acoustic backscatter at 40 kHz as a function of time after raking the sediment due to bioturbation. Figure 14 shows an example of changes of seafloor roughness, the two-dimensional roughness spectrum, and scattered level over time from the site discussed in Richardson et al.[18].

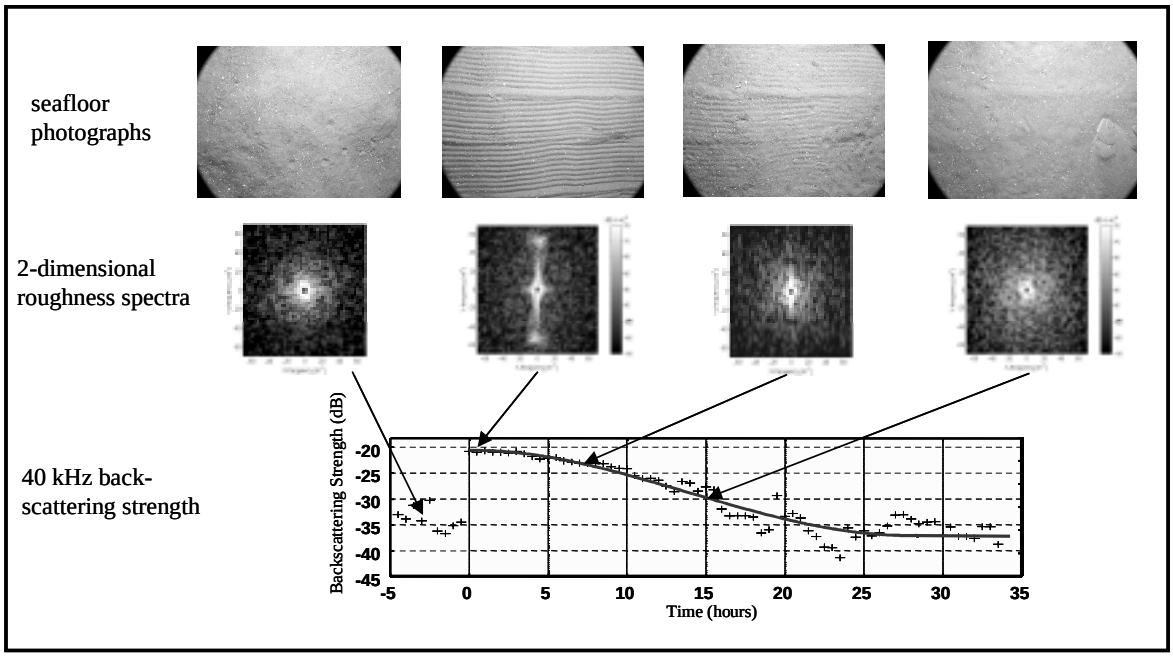

FIGURE 14. Time series seafloor photographs, two-dimensional roughness and 40 kHz backscattering taken during the SAX99 experiment at Panama City, Florida. Acoustic data are from Richardson, et al.[18].

3.4.3 Patchiness Studies

A common feature of shallow water seabeds is patchiness in properties, e.g., gravel or shell patches in the troughs of large ripples. For high-frequency acoustic systems designed for object detection a potentially important impact of these types of patchy seafloors is on scattered envelope statistics. In these types of environments, scattered envelope distributions can have significantly higher tails than a commonly assumed Rayleigh Distribution causing a higher than expected probability of false alarm[19]. Models have been developed recently attempting to link properties of the seafloor via seafloor scattering models to scattered envelope distributions[20,21,22]. Two-dimensional photogrammetry has the ability to provide inputs to these models such as the roughness properties of the patches and the size distribution of the patches. An example of non-stationarity or patchiness in roughness parameters is shown in Figure 15. In order to quantify the roughness properties of non-stationary roughness, the parameters of Equation (6) can be calculated on smaller portions of the height field (top right image in the figure) estimated from the original stereo photos (top left image). The spectral strength of Equation (6) is shown on the bottom left image of the figure and the spectral slope is shown on the bottom right. With this type of analysis the patchiness in roughness becomes evident.

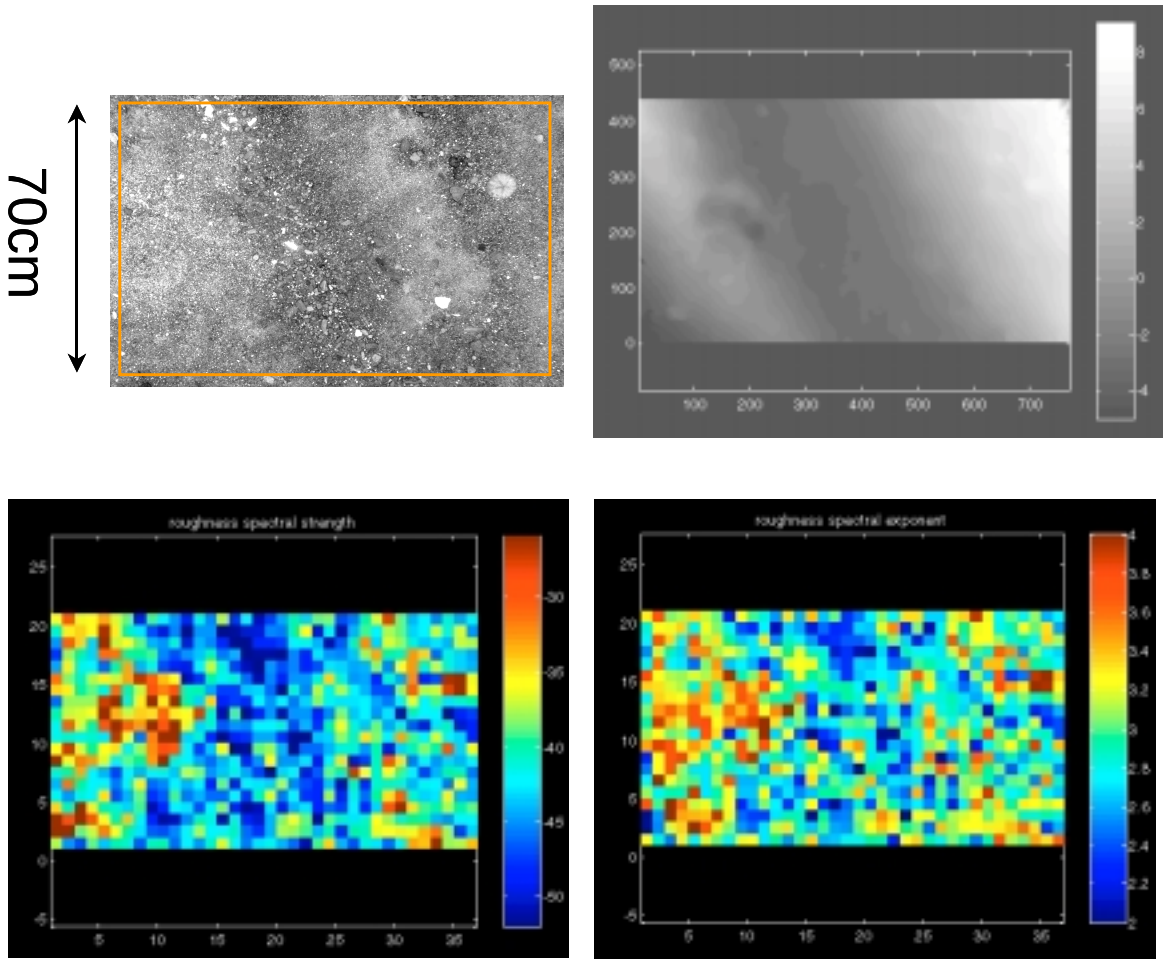

FIGURE 15. (top left) one photograph of a stereo pair taken of the seafloor near Halifax, Canada. (top right) Digital elevation model estimated from the stereo pair. (bottom left) Map of roughness spectral strength computed on sub regions. (bottom right) Map of roughness spectral exponent.

4 STUDYING ACOUSTIC PENETRATION USING BURIED DIRECTIONAL SENSORS

4.1 Overview

Understanding penetration into the sediment is necessary for any scenario where one would wish to obtain information from beneath the water sediment interface, such as detection of buried objects. The sediment penetration issue has been revisited recently by a number of investigators who have raised important questions about many long held assumptions. There have been repeated experiments recently[2,3] demonstrating "anomalous" penetration of acoustic energy into the seabed below the critical angle (i.e. above that predicted by elastic wave theory for smooth seabeds). Acoustic modeling and penetration experiments have suggested various causes for the anomalous penetration including a Biot "slow" compressional wave[2] and scattering from interface roughness[23]. Chotiros[2] used 20 kHz data obtained on a sparse buried hydrophone array to estimate the direction and speed of acoustic waves by intensity superposition that he interpreted as evidence of the Biot slow wave. Thorsos et al.[23] showed that acoustic scattering essentially straight down from the water sediment interface could also account for subcritical penetration and, additionally, for an array such as that used by Chotiros, the scattered signal could essentially mimic the slow wave. The fact that one cannot separate between the competing mechanisms of a Biot slow wave and an interface-scattered energy points out the difficulty in using sparsely distributed pressure sensors to measure the arrival angle of penetrating acoustic energy. Direct measurements of the arrival angle of acoustic energy penetrating the seafloor using accelerometers (or other types of vector sensors) should be able to conclusively separate between the two acoustic subcritical penetration mechanisms by illuminating not just *when* the energy arrives but *from where*. The refracted Biot slow wave (typical speed 1200-1300 m/s) would arrive from a grazing angle between approximately 30 and 45 degrees, while energy scattered by the rough water-sediment interface would come from almost directly above (i.e., around 90 degrees grazing angle). Thus estimates of the arrival angle of acoustic pulses could be used to separate the two mechanisms if the angle could be measured to within approximately 10 degrees.

A field trial has been performed to test the feasibility of using vector sensors such as accelerometers in studies of high-frequency acoustic penetration into sediments[24]. Uni-axial sensors, used for their sensitivity at high frequency, were used in orthogonal pairs during this experiment to determine arrival angles. In addition to sensitivity, one of the major questions addressed during the penetration experiment is the question of angular resolution. The main determinate of angular resolution for accelerometers is the off-axis sensitivity, i.e. what signal would be detected for a forcing orthogonal to the design sensing direction. The next section will give background into the issues relevant to the design of a accelerometer sensor package followed by examples of raw and processed data obtained using this novel technique.

4.2 Design Considerations

Several criteria governed the design of the buried directional receivers used in this study. The ideal receiver should have a high sensitivity to forcing on its axis of response, sufficient for example, to detect energy scattered downward from the seabed by a pulse incident at a shallow grazing angle. Meanwhile, in order to be effective at discriminating the angle of arrival of the energy, it should be relatively insensitive to off-axis forcing by translational motion, and to rotational motion, as this would manifest itself as a spurious on-axis translational component. It should be rigid within the frequency band of interest and thus free of any internal resonances. It should also be compact such that an orthogonal pair of receivers could be located within a fraction of an acoustic wavelength of each other in order to measure the acoustic field at that point in the seabed.

FIGURE 16. Pair of uni-axial accelerometers mounted to coupling disks. The sensors are attached to a burial jig using clips on the edges of the disks. Springs temporarily fix the clips to the inner, square, rod of the burial jig. The sensors are released when the rod is retracted.

The directional receiver that has been developed consists of an accelerometer fastened to a thin disk by a mounting stud (Figure 16). The disk ensures that it is well coupled and oriented in the medium in which it is emplaced. The system of an accelerometer and coupling disk will be referred to hereafter as an ACD. Specifying the dimensions and composition of a coupling disk is challenging as conflicting design requirements are encountered: maximum on-axis sensitivity requires minimal inertial mass; insensitivity to rotational motion requires maximum disk radius; minimizing internal resonances requires a thick disk with minimum radius; compact pair of sensors requires minimal disk radius. The mass of the coupling disk is approximately ten times that of the accelerometer, as per the manufacturers recommendation, and such that the accelerometer has a minimal effect on the motion of the object to which it is attached. The accelerometers were manufactured by Endevco Inc. and two versions of the same model were used, 7259A-25 and 7259A-100 with sensitivities of 25 and 100 mvg-1 respectively. They have a wide bandwidth with an amplitude response that is flat from 10 Hz to 50 kHz with a deviation of less than 1 dB. As they are not designed for underwater applications, the sensor housing and connection to the 1 mm diameter conducting cable had to be potted. This presented some difficulties, as the potting compound did not bond readily with the Teflon coating of the cable.

4.2.1 Example

In April and May 1999, two pairs of ACDs were deployed in a sandy sediment in a water depth of 12 m in Biodola Bay, Elba Island, Italy. Driven initially by penetration questions, the goals of the experiment included evaluating the feasibility of using vector sensors such as accelerometers in higher-frequency seafloor studies. Directional sources on a movable, telescopic tower and moored omni-directional sources transmitted pulses over a range of frequencies (2.5-29 kHz) at a variety of grazing angles: above critical for in situ calibration; at critical to study interaction of refracted and evanescent waves, and sub-critical to measure acoustic penetration into a sandy seafloor. The well-characterized site[4] had a sand layer thickness of approximately 2 m, a bulk density of 1920 kgm-3, and a compressional wave speed estimated at 1720 ms-1 (measured at 200 kHz from diver cores). The water sound speed was measured with a CTD to be 1530 ms-1, thereby creating a critical angle of approximately 29º. Burial of the ACD array was accomplished by the attaching the ACDs to a jig (also shown on Figure 15), releasing the ACDs once they are buried and the jig is retracted.

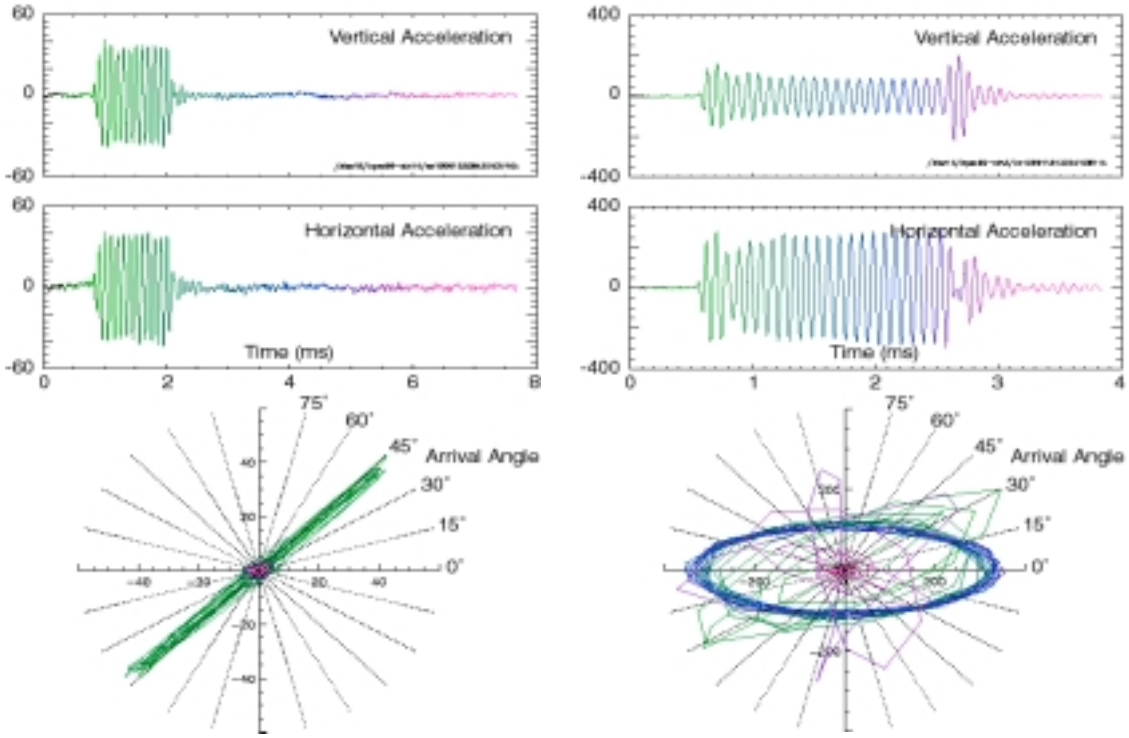

FIGURE 17. (left) Sample vertical and horizontal accelerations (top) measured on the ACDs at 50 cm depth for a 2 ms pulse of sound at 16 kHz, incident up the seabed at a grazing angle of 50^{o} and hodogram (bottom) displaying particle motion. The pulse is refraced to 42^{o}. (right) Same as for left but for a 2 ms pulse at 11 kHz incident at 30^{o}. The pulse is critically refracted to 0^{o}.

The vertical and horizontal acceleration of the ACDs in response to a pulse of sound (Figure 17, left) can be used to measure the angle of arrival by examining the orientation of the major axis of the elliptical motion produced by combining the separate components (Figure 17). The analysis can be repeated for different angles to measure arrival angle as a function of incident angle. The width of the minor axis of the ellipse indicates that some energy is not arriving in phase. (Phase quadrature between components would yield a circular particle motion.) The physical separation of the ACDs introduces a phase shift that one can correct as a function of frequency, but this requires some a priori knowledge about the angle of arrival and the properties of the seabed. However, phase shifts do not change the orientation of the major axis–they degrade the ability to discern it. Figure 17 also shows ACD measurements for a pulse transmitted below the critical angle. The evanescent wave can be clearly observed in this figure.

5 SUMMARY

Several applications of non-traditional technologies used to enhance studies of high-frequency seafloor acoustics have been discussed in this paper along with relevant examples. X-Ray computed tomography of seabed cores allows characterization of seabed properties at millimeter scales, as required by high-frequency acoustic volume-scattering modeling. This characterization included three dimensional continuum statistics of the sediment matrix and distributions of discrete scatterers. The sediment statistics can be cast in forms useful for constraining seafloor scattering models. The x-ray CT analysis also yields a greater insight into the geoacoustic parameters governing the nature of acoustic scattering from the seafloor. Inexpensive digital cameras and advances in personal computer-based photogrammetric processing of digital images have greatly improved our ability to quickly obtain quantitative, high-resolution, two-dimensional estimates of seafloor roughness. Ease of automation makes this technique an excellent candidate to support long-term studies of changes in acoustic response of the seafloor over time and could also

contribute to a better understanding of the dynamics of roughness, i.e., the formation and modification of microtopography due to bioturbation, currents or storm events. Vector sensors, such as accelerometers, appear to be a viable tool to study high-frequency penetration of acoustic energy into the sediment.

6 ACKNOWLEDGEMENTS

The author wishes to acknowledge a few of the host of people that had a hand in helping to develop the various systems and techniques presented in this paper. The seafloor acoustics group in the Department of Oceanography at Texas A&M University including A. Anderson, T. Orsi, and M. Duncan did much of the original work on validating and using x-ray CT scans on sediment cores. While at the NATO Undersea Research Centre (NURC), La Spezia, Italy, the author collaborated with E. Pouliquen and L. Muzi on the later x-ray CT work presented here. The digital photogrammetry system was developed at NURC with the encouragement and support of T. Akal and N. Pace. The accelerometer system design and calibration, experimental data collection, and data analysis were done jointly with J. Osler of Defence R&D Canada.

7 REFERENCES

1. E. Pouliquen and A.P. Lyons, Backscattering from bioturbated sediments at very high frequency, IEEE J. Ocean. Eng., 27, 388-402. (2002).
2. K.L Williams, D.R. Jackson, E.I. Thorsos, D. Tang, and K.B. Briggs, Acoustic backscattering experiments in a well characterized sand sediment: data/model comparisons using sediment fluid and Biot models, IEEE J. Ocean. Eng., 27, 376-387. (2002).
3. N.P. Chotiros, Biot model of sound propagation in water-saturated sand, J. Acoust. Soc. Amer., 97, 199-214. (1995).
4. A. Maguer, W. L. J. Fox, H. Schmidt, E. Pouliquen, and E. Bovio, Mechanisms for subcritical penetration into a sandy bottom: experimental and modelling results, J. Acoust. Soc. Amer., 107, 1215-1225. (2000).
5. G.N. Hounsfield, Computerized transverse axial scanning (tomography): part 1. Description of system, Brit. J. Radiology, 46, 1016-1022. (1973).
6. G.S. Warner, J.L. Nieber, I.D. Moore, and R.A. Geise, Characterizing macropores in soil by computed tomography, Soil Sci. Soc. Am. J., 53, 653-660. (1990).
7. A.P. Lyons, M.E. Duncan, J.A. Hawkins and A.L. Anderson, Predictions of the acoustic scattering response of free methane bubbles in muddy sediments, J. Acoust. Soc. Am., 99, 163-172. (1996).
8. A.L. Anderson, F. Abegg, J.A. Hawkins, M.E. Duncan and A.P. Lyons, Bubble populations and acoustic interaction with the gassy Floor of Eckernförde Bay, Continental Shelf Res., 18, 1807-1838. (1998).
9. A.P. Lyons, Modeling high-frequency seafloor volume backscatter by shell fragment distributions, Proc. of the Sixth International Conference on Theoretical and Computational Acoustics. Honolulu, Hawaii (2003).
10. L.M. Cruz-Orive, Distribution-free estimation of sphere size distributions from slabs showing overprojection and truncation, with review of previous methods, J. Microsc., 131, 235-244. (1982).
11. T.H. Orsi, A.L. Anderson and A.P. Lyons, X-Ray tomographic analysis of sediment macrostructure in Eckernförde Bay, western Baltic Sea, Geo-Marine Letters, 16, 232-239. (1996).
12. A.P. Lyons and T.H. Orsi, The effect of a layer of varying density on high-frequency reflection, forward loss, and backscatter, IEEE J. Ocean. Eng., 23, 411-422. (1998).
13. L. Muzi, A.P. Lyons and E. Pouliquen, Use of x-ray computed tomography for the estimation of parameters relevant to the modeling of acoustic scattering from the seafloor, Nucl. Instr. and Meth. in Phys. Res. B, 213, 491-497. (2002).

14. A.P. Lyons, A.L. Anderson, and F.S. Dwan, Acoustic Scattering from the seafloor: modelling and data comparison, J. Acoust. Soc. Am., 95, 2441-2451. (1994).
15. D.R. Jackson, K.L. Williams, E.I. Thorsos, and S.G. Kargl, High-frequency subcritical penetration into a sandy sediment, IEEE J. Oceanic Eng., 27, 346-361. (2002).
16. J.E. Piper, K.W. Commander, E.I. Thorsos, and K.L. Williams, Detection of buried targets using a synthetic aperture sonar, IEEE J. Oceanic Eng., 27, 495-504. (2002).
17. A.P. Lyons, W.L.J. Fox, T. Hasiotis and E. Pouliquen, Characterization of the two-dimensional roughness of shallow-water sandy seafloors, IEEE J. Ocean. Eng., 27, 515-524. (2002).
18. M.D. Richardson, K.B. Briggs, K.L. Williams, A.P. Lyons and D.R. Jackson, Effects of changing roughness on acoustic scattering: anthropogenic roughness, in Proc. of the Inst. of Acoust., 23, 201-208. (2001).
19. A.P. Lyons and D.A. Abraham, Statistical characterization of high-frequency shallow-water seafloor backscatter, J. Acoust. Soc. Am., 106, 1307-1315. (1999).
20. D.A. Abraham and A.P. Lyons, Novel physical interpretations of K-distributed reverberation, IEEE J. Ocean. Eng., 27, 800-813. (2002).
21. A.P. Lyons, D.A. Abraham and E. Pouliquen, Predicting scattered envelope statistics of patchy seafloors, in N.G. Pace and F.B. Jensen, eds., Impact of Littoral Environmental Variability on Acoustic Predictions and Sonar Performance, Kluwer Academic Publishers, Netherlands, 211-218. (2002).
22. D.A. Abraham and A.P. Lyons, Reverberation envelope statistics and their dependence on sonar bandwidth and scatterer size, IEEE J. Ocean. Eng., in press. (January 2004)
23. E. I. Thorsos, D. R. Jackson, and K. L. Williams, Modeling of subcritical penetration into sediments due to interface roughness, J. Acoust. Soc. Am., 107, 263-277. (2000).
24. J.C. Osler and A.P. Lyons, High-frequency seafloor studies using buried directional receivers, Proc. of the High Freq. Ocean Acoust. Conf. La Jolla, CA (2004).